Eur. Phys. J. Special Topics **223**, 2475–2481 (2014)

DOI: 10.1140/epjst/e2014-02216-9

THE EUROPEAN PHYSICAL JOURNAL SPECIAL TOPICS

Regular Article

Emergence of a phase transition for the required amount of storage in highly renewable electricity systems

Tue Vissing Jensen[1,2,a] and Martin Greiner[3,b]

[1] Department of Electrical Engineering, Technical University of Denmark, Richard Petersens Plads 325, 2800 Kongens Lyngby, Denmark
[2] Department of Physics and Astronomy, Aarhus University, Ny Munkegade 120, 8000 Aarhus C, Denmark
[3] Department of Engineering and Department of Mathematics, Aarhus University, Ny Munkegade 118, 8000 Aarhus C, Denmark

Received 26 April 2014 / Received in final form 14 May 2014
Published online 24 June 2014

Abstract. Due to global environmental concerns, our electricity supply will transform from mostly conventional power generation to mostly fluctuating renewable power generation. The transition will require combined backup from conventional sources and storage. A phase transition emerges during the ramp-up of the required amount of storage, with renewable penetration being the control parameter and average relative storage filling level being the order parameter. A singularity appears for the required storage energy capacity at a renewable penetration determined by the parameters of the storage. For an ideal storage with no roundtrip losses the transition occurs at 100% renewable penetration. Moreover, the required storage energy capacity is strongly enhanced by temporal correlations on the synoptic weather time scale. A Markov process is proposed, which reproduces these findings.

1 Introduction

Intermittent renewable energy technologies are already an important part of our energy system, and their role in covering energy demand will only increase in the future, pushed by a global agenda to decrease emissions and reliance on fossil fuels. Recent research has examined a possible end-point of this transition: a fully renewable energy system based on wind, solar and water power [1–4]. System engineering based on the physics of complex systems is needed to design such far-future energy infrastructures, whose dynamics are driven by fluctuating spatio-temporal weather patterns. Based on state-of-the-art high-resolution meteorological data, several fundamental properties of a fully renewable pan-European electricity system have already been derived. Amongst such characteristics are the optimal mix between wind and solar

[a] e-mail: tvjens@elektro.dtu.dk
[b] e-mail: greiner@eng.au.dk

power generation [5,6], the optimal synergies between storage and balancing [7], the optimal extension of the transmission network [8–11], and the interplay between grid and storage [12]. These findings on the design of far-future energy systems provide important guidance for the design of near-future energy networks. Forward pathways from the presence into the near future can be matched with backward pathways from the far future into the near future to thoroughly design and execute the challenging "Energiewende".

This Paper focuses on the required need for storage in near- and far-future electricity systems, as seen from a more general and fundamental perspective. In Refs. [6,7,13,14] it has been observed, that in highly renewable electricity systems the need for storage at first strongly increases with the renewable penetration in a nonlinear way, only then to strongly decrease again once a critical penetration has been passed. It has been speculated that the emergence of this cusp singularity might be related to a phase transition [7]. Based on renewable power generation data and historical load [5], a simple time-series model describing the storage filling level is discussed in Sect. 2. With increasing renewable penetration a sudden transition from a low-storage-filling-level phase to a high-storage filling level phase is found to occur at a critical penetration, which causes a singular behavior for the storage energy capacity. Compared to randomized renewable power generation data, which is treated in Sect. 3, temporal correlations on the synoptic weather time scale cause a strong increase for the required storage energy capacity. A Markov process is proposed in Sect. 4, which reproduces the storage size requirements found in the data. The conclusion is given in Sect. 5.

2 Data-driven time series modeling of the storage dynamics

The key to the construction of a simple storage model is the mismatch

$$\Delta(t) = \gamma G_{\mathrm{RES}}(t) - L(t) \tag{1}$$

between the renewable power generation $\gamma G_{\mathrm{RES}}(t)$ and the load $L(t)$ at some instance t in some region. For convenience, the normalization is such that the temporal averages are $\langle G_{\mathrm{RES}}(t)\rangle = \langle L(t)\rangle = 1$. The parameter γ describes the penetration of average renewable power generation. When γ is smaller/equal/larger than one, the average renewable power generation is smaller/equal/larger than the average load, and consequently the average mismatch is smaller/equal/larger than zero.

The underlying mismatch time series (1) has been constructed from a recently developed renewable energy atlas; for more details see [5]. Here, the renewable power generation

$$G_{\mathrm{RES}}(t) = \alpha G_{\mathrm{WIND}}(t) + (1-\alpha) G_{\mathrm{SOLAR}}(t) \tag{2}$$

is defined as the combined wind and solar power generation with a mixing factor of $\alpha = 0.6$, and has been aggregated over 27 European countries. The specific choice $\alpha = 0.6$ leads to a seasonal detrending of the mismatch (1) around $\gamma = 1$ [5]. We assume that the European transmission network is sufficiently strong as to not constrain the sharing of renewables [10].

For ease of discussion, we assume an ideal storage, with charging and discharging efficiencies $\eta_+ = \eta_- = 1$ and no constraints on the charging and discharging powers. It is straightforward to formulate a dynamical model for the storage filling level:

$$f(t) = \begin{cases} \max(f(t-1) + \Delta(t), 0) & (\text{for } \gamma < 1) \\ f(t-1) + \Delta(t) & (\text{for } \gamma = 1) \\ \min(f(t-1) + \Delta(t), 0) & (\text{for } \gamma > 1), \end{cases} \tag{3}$$

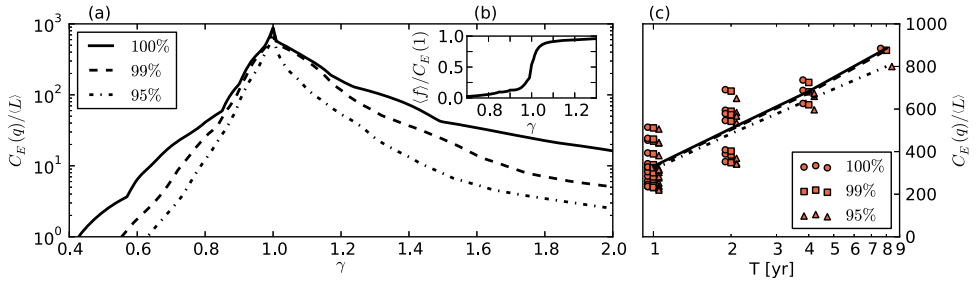

Fig. 1. (a) Storage energy capacity based on the quantiles $q = 1.00, 0.99, 0.95$ as a function of the renewable penetration γ. The mismatch data has been taken from a recently developed European Renewable Energy Atlas [5]. The storage energy capacity is measured in units of the average hourly load. (b) γ-dependence of the average storage filling level divided by the respective $q = 1.00$ storage energy capacity. (c) For the case $\gamma = 1.0$, dependence of the storage energy capacity on the length T of the mismatch time series. Lines indicate the mean over ensemble for each quantile.

where the division into three cases based on γ ensures the average storage filling level to remain bounded. A periodic boundary condition $f(0) = f(T)$ is imposed in order to keep the storage neutral [7]. For $\gamma > 1$, $f(t)$ is negative, which is purely for notational convenience; shifting $f(t)$ by $|\min_t(f(t))|$ after calculation allows direct comparison of storage level time series. In this simple model, storage is used as much as possible and as much as needed. For $\gamma < 1$ the storage is filled as much as possible, but storage alone is not sufficient to serve all occuring negative mismatches. Once the storage runs empty, additional backup power generation is needed. For $\gamma > 1$ no backup is needed, but the storage is filled only as much as needed. The remainder of the positive mismatches is curtailed.

Over a sufficiently long time T with $\gamma \neq 1$, the dynamics (3) produces a stationary γ-dependent distribution $p(f)$ for the storage filling level. Its quantiles are defined by $q = \int_{f_{\min}}^{Q} p(f)df$ and determine the storage energy capacity:

$$C_{\mathrm{E}}(q) = \begin{cases} Q(q) & (\text{for } \gamma < 1) \\ Q(\frac{1+q}{2}) - Q(\frac{1-q}{2}) & (\text{for } \gamma = 1)\ . \\ -Q(1-q) & (\text{for } \gamma > 1) \end{cases} \tag{4}$$

A quantile-based definition is used for ease of comparison with the stochastic mismatch models introduced later.

Figure 1a illustrates the resulting γ-dependence of the storage energy capacity based on three different high quantiles. Note the logarithmic scale on the y-axis. As γ increases from $\approx$0.5 to 1, the storage energy capacity increases by three orders of magnitude, only then to decrease again by more than two orders of magnitude as γ approaches 2. Figure 1b illustrates the average relative storage filling level as a function of γ. There is a relatively sharp transition from a low filling level (floor phase) for $\gamma < 1$ to a high filling level (ceiling phase) for $\gamma > 1$. These features are precisely what would be expected for a phase transition with γ as the control parameter and the average relative storage filling level as the order parameter. Exactly at $\gamma = 1$ the system does not know to which phase to belong to, and the storage energy capacity should become singular. The finite peak in Fig. 1a would then be a finite size effect, rather than an intrinsic property of the system. Figure 1c reveals how the storage energy capacity at $\gamma = 1$ changes when the eight years of data have been chopped

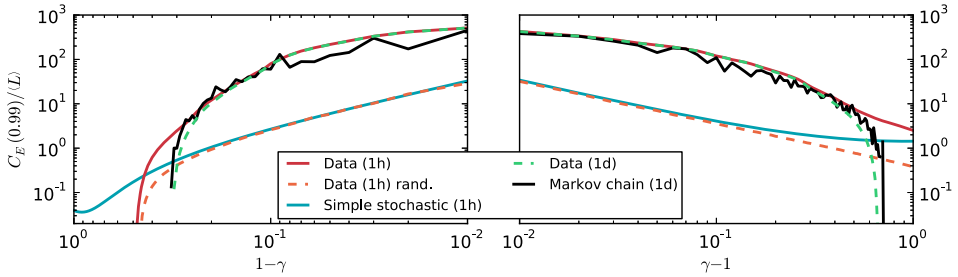

Fig. 2. Storage energy capacity based on the $q = 0.99$ quantile as a function of $|\gamma - 1|$. The different curves correspond to the hourly European Renewable Energy Atlas data (solid red), the randomized hourly data (dashed orange), the simple hourly stochastic model (6)–(8) (solid blue), the daily data (dashed green) and the Markov model derived from the transition probability for the daily mismatches (solid black).

into one-, two- and four-year segments. The mean of these estimates grows with the segment length, and does not seem to converge to a finite value, indicating that the length of the data set is insufficient to reveal details close to $\gamma = 1$.

Due to the finiteness of the storage energy capacity at $\gamma = 1$, it is difficult to extract a scaling law of the form

$$C_{\mathrm{E}} \sim \frac{1}{|\gamma - 1|^{\delta}}. \tag{5}$$

In fact Fig. 2 reveals that there is no such rigorous scaling law around $\gamma = 1$. In the following we will show that this finding is due to temporal correlations in the mismatch time series which are caused by the dominant weather time scales.

3 Temporal randomization

A randomization of the mismatch time series (1) leads to the dashed orange curve in Fig. 2. The removal of the temporal correlations leads to a clear scaling law (5) with exponent $\delta = 1.0$. This can be understood analytically. The temporal evolution (3) of the storage filling level can be expressed to some approximation as a stochastic differential equation

$$df = A dt + \sqrt{B} d\Gamma \tag{6}$$

with a reflecting boundary condition at the storage floor or ceiling, respectively. The Gaussian white noise Γ comes with unit variance. The first two cumulants of the mismatch distribution determine the drift and diffusion coefficients

$$\begin{aligned} A &= \gamma - 1, \\ B &= \gamma^2 \left(\left\langle G_{\mathrm{RES}}^2 \right\rangle - 1 \right) - 2\gamma \left(\langle G_{\mathrm{RES}} L \rangle - 1 \right) + \left(\left\langle L^2 \right\rangle - 1 \right). \end{aligned} \tag{7}$$

Note, that due to the dominant moment $\left\langle G_{\mathrm{RES}}^2 \right\rangle$, attributed to the greater variability of the generation, the diffusion coefficient goes as $B \sim \gamma^2$ for $\gamma \gtrsim 0.4$. The stationary probability distribution for this process with a reflecting boundary at $f = 0$ is $p(f) = |A/2B| \exp(Af/2B)$ [15]. Its quantiles determine the storage energy capacity (4), which then becomes for $\gamma \neq 1$:

$$C_{\mathrm{E}}(q) = \left| \frac{2B}{A} \right| \ln \left(\frac{1}{1-q} \right). \tag{8}$$

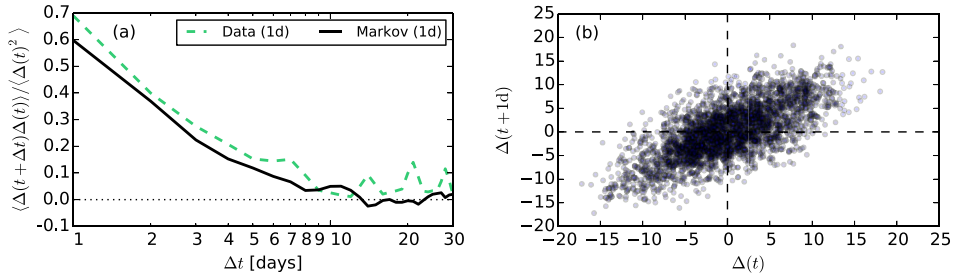

Fig. 3. (a) Autocorrelation of the daily mismatch, derived from daily aggregate data (dashed curve) and from the Markov-chain model (solid curve) for $\gamma = 1.0$ and $\alpha = 0.6$. (b) Scatter plot for consecutive daily mismatches in units of the average hourly load for $\gamma = 1.0$ and $\alpha = 0.6$.

For γ close to one, this leads to the scaling law (5) with exponent $\delta = 1$. The expression (8) produces the blue curve in Fig. 2, and agrees nicely with the curve for the randomized data.

4 Temporal correlations

The autocorrelation of the mismatch is shown in Fig. 3a. A one-day aggregation of the mismatch has been used in order to detrend the regular intra-day pattern introduced by the solar power generation $G_{\mathrm{SOLAR}}(t)$ and the load $L(t)$. As shown in Fig. 2, this aggregation has no effect on the storage energy capacity for γ close to one. The correlation time is of the order of one week and matches nicely with the synoptic time scale of the weather. Note that the seasonal time scale does not contribute here due to the specific choice $\alpha = 0.6$ in (2).

The correlation is also visible in Fig. 3b, which shows the daily mismatch as a function of the previous value. The stretched cloud expresses a positive correlation between two successive mismatch values. This scatter plot also allows the extraction of the transition probability $p(\Delta(t+1)|\Delta(t))$. The estimation is done nonparametrically using the Epanechnikov kernel, a well-studied kernel with compact support that is common in applications [16]. The kernel bandwidths are chosen using the rules of thumb for Gaussian marginals given in [16]. The estimated transition probability allows to model the temporal evolution of the mismatch as a Markov chain. Simulations of the resulting time series are then used to derive estimates for the storage energy capacity according to (3) and (4). These estimates are also shown in Fig. 2, and agree within fluctuations with the results obtained from the hourly and daily mismatch data.

It is the temporal correlations of the mismatch which lead to a deviation from the scaling law (5). They also cause a strong increase of the storage energy capacity; compare again the topmost curves of Fig. 2 with the bottom two, which are more than one order of magnitude apart from each other. Since the temporal mismatch correlations are dominated by the synoptic time scale of the weather, it is also this time scale which is in charge of the strong increase in required storage energy capacity. The intra-day time scales do not play a big role. This can be concluded in two ways: first, the storage energy capacity derived from the hourly mismatches is almost identical to its counterpart derived from daily mismatches; see again Fig. 2. Second, the required storage energy capacity for intraday mismatch fluctuations is of the order of the load consumed in 6–12 hours. Compared to the storage energy capacity of about 4–5 load weeks found for renewable penetrations around $\gamma \approx 1$, this is two orders of

magnitude smaller; see again Figs. 1 and 2. Note that if the seasonal time scale had not been removed with the specific choice $\alpha \approx 0.6$ for the mixing factor in (2), or if the underlying transmission network had not been assumed to be sufficiently strong, the resulting storage energy capacity would have been even greater than the energy contained in 4–5 load weeks [6].

Relaxing the assumption of ideal storage efficiencies does not impact the above discussion. Only the critical penetration changes: for efficiencies $\eta_+, \eta_- < 1$, the critical penetration will shift from $\gamma = 1$ to the solution of the implicit equation $\gamma = 1 + ((\eta_-\eta_+)^{-1} - 1)B(\gamma)$, where $B(\gamma) = -\langle \min(\Delta(\gamma), 0)\rangle$.

5 Conclusion

The preceding analysis indicates, that an electricity system built with renewable penetration close to 100% will require extremely large storage capacities if storage is to play a major part in balancing the system. These capacities will be much larger than what is currently discussed with existing and prospected pumped hydro, compressed air and hydrogen facilities, with electro-chemical batteries or with demand-side management in smart grids. Economically and operationally it will be smarter to design the future electricity system away from a 100% penetration of renewables, where less storage is needed. Either the system should be constructed for less penetration, keeping a larger portion of conventional power generation, or the penetration should be increased above 100%.

In the latter case, the excess renewable penetration does not need to be extremely large. Ref. [7] has shown that in the limit of a sufficiently strong transmission grid the excess penetration of a European electricity system amounts to only 17% once an ideal battery storage with an energy capacity corresponding to six load hours is complemented by the green hydro and biomass backup resources already available today. If in addition also a hydrogen storage with non-ideal roundtrip efficiencies and with an energy capacity corresponding to 2,5 load days is taken into account, then the excess penetration would further reduce down to 5% only.

Excess renewable penetration in an electricity system leads of course to massive excess renewable power generation. This does not necessarily represent a drawback. The excess renewable power generation does not need to be curtailed. Instead, it could be used to partially electrify the other two energy sectors, namely heating and transportation. Given this perspective, excess renewable penetration could on purpose be increased even further, thus leading all the way to a fully sustainable smart network of strongly coupled energy infrastructure networks, including also a new design of future energy markets.

The authors would like to thank G. Andresen, S. Becker, A. Søndergaard and M. Rasmussen for several fruitful discussions.

References

1. M.Z. Jacobson, M.A. Delucchi, Scientific Amer. **301**, 58 (2009)
2. M.Z. Jacobson, M.A. Delucchi, Energy Policy **39**, 1154 (2011)
3. M.Z. Jacobson, M.A. Delucchi, Energy Policy **39**, 1170 (2011)
4. H. Lund, *Renewable Energy Systems – The Choice and Modeling of 100% Renewable Solutions* (Elsevier, Amsterdam, 2010)
5. D. Heide, L.v. Bremen, M. Greiner, C. Hoffmann, M. Speckmann, S. Bofinger, Renewable Energy **35**, 2483 (2010)

6. D. Heide, M. Greiner, L.V. Bremen, C. Hoffmann, Renewable Energy **36**, 2515 (2011)
7. M.G. Rasmussen, G.B. Andresen, M. Greiner, Energy Policy **51**, 642 (2012)
8. K. Schaber, F. Steinke, P. Mühlich, T. Hamacher, Energy Policy **42**, 498 (2012)
9. K. Schaber, F. Steinke, T. Hamacher, Energy Policy **43**, 123 (2012)
10. R.A. Rodriguez, S. Becker, G.B. Andresen, D. Heide, M. Greiner, Renewable Energy **63**, 467 (2014)
11. S. Becker, R.A. Rodriguez, G.B. Andresen, S. Schramm, M. Greiner, Energy **64**, 404 (2014)
12. F. Steinke, P. Wolfrum, C. Hoffmann, Renewable Energy **50**, 826 (2013)
13. M. Popp, *Speicherbedarf bei einer Stromversorgung mit Erneuerbaren Energien* (Springer, Heidelberg, 2010)
14. C. Budischak, D. Sewell, H. Thomson, L. Mach, D.E. Veron, W. Kempton, J. Power Sources **225**, 60 (2013)
15. C.W. Gardiner, *Handbook of Stochastic Methods* (Springer, Berlin, 1983)
16. D.M. Bashtannyk, R.J. Hyndman, Comput. Stat. Data Anal. **36**, 279 (2001)